

HIGH DENSITY CIRCULATING FLUIDIZED BED RISER: INFLUENCE OF DRAG MODEL, KINETIC THEORY AND WALL SLIP CONDITIONS

Damian Ramajo^a, Santiago Marquez Damian^a, Marcela Raviculé^b and Norberto Nigro^a

^a*International Center for Computational Methods in Engineering (CIMEC)
INTEC-UNL-CONICET, Güemes 3450 S3000GLN Santa Fe, Argentina
dramajo@santafe-conicet.gov.ar*

^b*Centro de Tecnología Argentina (CTA), YPF, Baradero s/nro. 1925, Ensenada, Argentina
mravicules@ypf.com*

Keywords: CFD, Circulating Fluidized Bed, Drag Model, Kinetic Theory of Granular Flow

Abstract. High density circulating fluidized bed (HDCFB) modeling has been performed by Computational Fluid Dynamics (CFD). The influence of three crucial modeling parameters was studied; the drag model (the Wen Yu, Gidaspow and EMMS models were assessed), the use of kinetic theory of granular flow (KTGF) and the wall slip condition (influence of slip, no slip and partially slip boundary conditions were investigated). Comparison of numerical results with experimental ones reported in literature for a laboratory planar riser allowed pointing out the impact of each one of the three modeling parameters on flow behavior, concluding that the drag model has a crucial role on the prediction of solid output flow and solid vertical profile. On the other hand, KTGF and the no-slip wall condition showed to be crucial to guaranty the numerical stability.

1 INTRODUCTION

Circulating fluidized bed (CFB) is widely used in industrial applications like cracking, drying, catalyst regeneration in FCC units and combustion (Grace et al., 2003). The complex interaction between solid and gas phases and solid-solid particles in the risers presents a tangible challenge to the improvement and understanding of fluidized bed systems (Gauthier, 2009).

Computational fluid dynamics (CFD) model for gas-solid two-phase systems can be grouped in Eulerian-Lagrangian and Eulerian-Eulerian models.

Eulerian-Lagrangian models allow to describe the fluid-particle (eg. drag and non-drag forces), particle-particle (eg. collisions and friction) and particle-wall interaction. But, today with the current most powerful computer systems the number of particles that can be tracked with these models is far to be closer to the required for fluidized bed problems (Wang et al., 2007).

On the other hand, in the Eulerian-Eulerian models, gas and solid are described as interpenetrating continua. Although Eulerian-Eulerian models are massively employed to carry out parametric and scale-up and design studies, there is still no consensus on the treatment of the solid-phase viscosity, solid stress modulus and particle restitution coefficients. All these particle-particle interaction parameters have fundamental importance for high density fluidized gas-solid systems but relatively poor influence when solid volume fraction keeps less than 0.15. But for diluted gas-solid systems, gas-particle interaction (drag forces) gets crucial for correct modeling. In this sense, recent papers had faced the more used drag models versus experimental data (Yang et al., 2003; Cruz et al., 2006; Almuttahir and Taghipour, 2008; Zhang et al., 2008; Hartge et al., 2009; Wang et al., 2010).

In this work, a comparative study between three drag models; Wen and Yu, Gidaspow and energy-minimization multi-scale (EMMS) models are compared with experimental riser data from literature (Yang et al, 2003). The kinetic theory of granular flow KTGF is also assessed and the influence of the wall boundary condition (WBC) is evaluated for no-slip, free-slip and partial free-slip situations.

2 METHODOLOGY

2.1 Computational model

Figure 1 shows the planar riser configuration employed and the boundary conditions associated. Due to software requirements, one grid element had to be used at z direction in order to obtain a three dimensional model. However, in this direction all variables are considered constants, setting a symmetry wall boundary condition at the front and back surfaces.

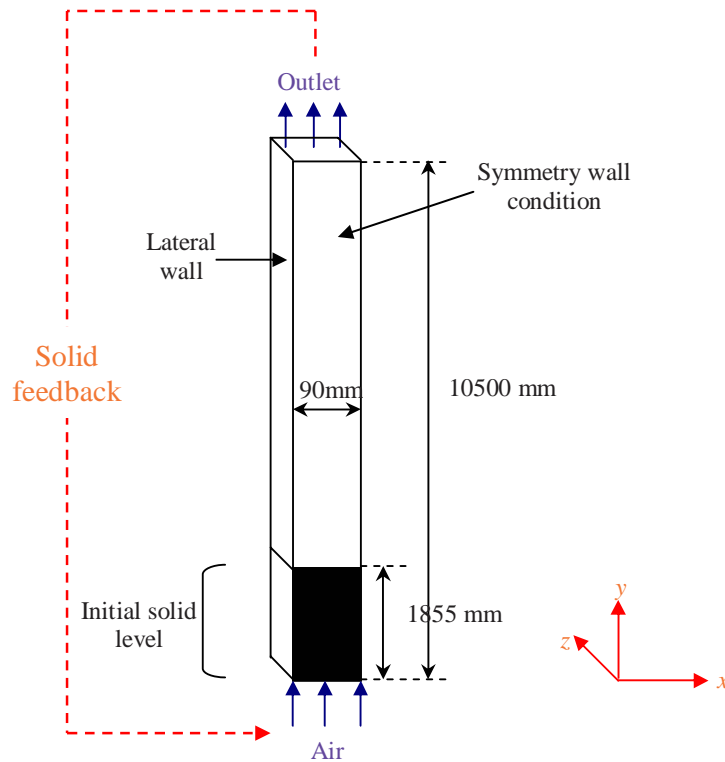


Figure 1: Computational domain

Three structured grids were generated by means of Octave in order to represent a laboratory planar riser. Grids were essentially 2-dimensional with only one element in the z direction. Table 1 describes the grid characteristics. The second one is the same that was employed for Yang et al. (2003), while the other two grids were added in order to perform a mesh convergence analysis.

Grid	Divisions (x)	Divisions (y)	Divisions (z)	Nodes	Elements
G ₁	30	200	1	6231	6000
G ₂	40	300	1	12341	12000
G ₃	50	400	1	20451	20000

Table 1: Grids characteristics

An inlet boundary condition was employed at the bottom of the riser. Air was injected with a homogeneous constant velocity of 1.52 m/s. The solid mass flow rate was monitored at the top outlet and automatically reentered through the bottom inlet to represent the laboratory circulating fluidized bed (CFB). The front and back walls were modeled as symmetry boundaries (free slip condition) in order to better represent the thickness laboratory riser by the 2-dimensional grid. Three boundary conditions were implemented for the lateral walls at the left and right:

- a- no-slip for air and solid
- b- free-slip for air and solid
- c- partial free-slip (no-slip for air and free-slip for solid).

Simulations were transients with a constant time step defined by a time convergence study. Initial conditions were a solid column of 1855 mm with a volume fraction of 0.4 and zero velocity for both phases.

The two-fluid model was employed to model both air and solid particles. Air was represented as a continuous phase with constant properties at room temperature while solid phase was modeled as discrete particles of 54 μm .

2.2 Governing equations

The unsteady Eulerian-Eulerian two-fluid model implemented in the finite volume commercial software ANSYS-CFX 12.0 was employed for simulations. As it is well known from theory (Drew and Passman, 1998), in this formulation the single phase Navier-Stokes equations (N-S) are modified according to some sort of regularization or average to model the small scales, introducing the volume fraction of each phase along with appropriate terms considering the mass, momentum and energy transferred through the interface among phases.

Gas phase was considered as incompressible, because compressible effects are not significant at low velocity (Mach number less than 0.2). The continuity equation for gas and solid phases is:

$$\begin{aligned} \frac{\partial}{\partial t}(\delta_g \rho_g) + \nabla \cdot (\delta_g \rho_g \vec{u}_g) &= 0 \\ \frac{\partial}{\partial t}(\delta_s \rho_s) + \nabla \cdot (\delta_s \rho_s \vec{u}_s) &= 0 \end{aligned} \quad (1)$$

where δ is the volume fraction, ρ the density and \vec{u} the velocity.

Summation of the volume fraction δ of all phases must be 1, being a constraint condition:

$$\sum_i \delta_i = 1 \quad \text{with } i = g, s \quad (2)$$

Regarding the momentum equation, it can be written as:

$$\begin{aligned} \frac{\partial}{\partial t}(\delta_g \rho_g \vec{u}_g) + \nabla \cdot (\delta_g (\rho_g \vec{u}_g \vec{u}_g)) &= -\delta_g \nabla P + \nabla \cdot \bar{\bar{\tau}}_g + \delta_g \rho_g \vec{g} + K_{sg} (\vec{u}_s - \vec{u}_g) \\ \frac{\partial}{\partial t}(\delta_s \rho_s \vec{u}_s) + \nabla \cdot (\delta_s (\rho_s \vec{u}_s \vec{u}_s)) &= -\delta_s \nabla P - \nabla P_s + \nabla \cdot \bar{\bar{\tau}}_s + \delta_s \rho_s \vec{g} + K_{sg} (\vec{u}_g - \vec{u}_s) \end{aligned} \quad (3)$$

where P is the static pressure, P_s is the solid pressure, τ is the shear stress tensor and K_{sg} is the interface momentum exchange coefficient (drag force). In this work, only drag forces were considered due to non-drag forces only become significant for liquid-bubble systems. Problem was assumed as isothermal, so the energy equation was not solved.

The standard two equation k - ε model was employed to model turbulence and a standard logarithmic wall law was applied to represent the logarithmic velocity profile near walls, thus avoiding high mesh refinement. k - ε model has been extensively employed to simulate multiphase systems due to its robustness and accuracy even with relatively rough meshes (Ranade, 2002; Ramajo et al., 2008).

Regarding time integration, a first order Backward Euler scheme was applied. A range of time steps from 1×10^{-3} s. to 5×10^{-4} s. were studied. For the two drag models available in Software (Wen and Yu and Gidaspow) it was possible to use a time step of 5×10^{-3} s., guarantying stability and root mean square (RMS) convergence criterion for residual less than 1×10^{-6} . However, instabilities were found for the own EMMS implementation, so the time step was reduced to 5×10^{-4} . Equations were solved using distributed computing facilities over several processors in a Beowulf cluster.

The use of kinetic theory of granular flow (KTGF) for solving gas-solid systems had been extensively implemented in the recent years becoming the typical modeling choice. There are at least three particle-particle interaction mechanisms popularly accepted; the kinetic, the collisional & kinetic and the frictional model. The employed software only incorporates models for the first two mechanisms, being the last one the more significant for high density gas-solid systems. The background and general theory of the KTGF has been extensively reported and discussed in literature (Huilin et al., 2003, Gidaspow, 1994). The specific equations solved in this work can be consulted in ANSYS-CFX 12 User Manual, 2008.

2.2.1 Drag models

Three drag models were assessed; the Wen and Yu, the Gidaspow and the EMMS models. The interface momentum exchange coefficient K_{sg} for Wen and Yu is:

$$K_{sg} = \frac{3(1-\delta_g)\delta_g}{4d_p} \rho_g |u_g - u_s| C_{D0} \delta_g^{-2.7} \quad \text{for } \forall \delta_s \quad (4)$$

where C_{D0} is the drag coefficient for a isolated particle immersed in a laminar fluid:

$$C_{D0} = \left(0.63 + \frac{4.8}{\sqrt{\text{Re}_p}} \right)^2 \quad (5)$$

being the particle Reynolds number:

$$\text{Re}_p = \frac{\delta_g \rho_g |\vec{u}_g - \vec{u}_s| d_p}{\mu_g} \quad (5)$$

In Eq. (6) d_p is the particle diameter and μ_g the dynamic viscosity of gas. The Gidaspow drag model employs the Wen and Yu model (Eq. (4)) for dilute systems ($\delta_s < 0.2$) and the Ergun correlation for porous media for dense systems:

$$K_{sg} = 150 \frac{(1-\delta_g)^2 \mu_g}{\delta_g d_p^2} + 1.75 \frac{(1-\delta_g) \rho_g |u_g - u_s|}{d_p} \quad \text{for } \delta_s \geq 0.2 \quad (6)$$

The EMMS model is a variation of the Gidaspow one, also using the Ergun correlation (eq. (6)) for dense systems (solid volume fraction higher than 0.26 in this case) and adding a correction coefficient ϖ at the Wen and Yu model for dilute systems:

$$\begin{aligned}
 K_{sg} &= \frac{3(1-\delta_g)\delta_g}{4d_p} \rho_g |u_g - u_s| C_{DO} \varpi && \text{for } \delta_s \leq 0.26 \\
 K_{sg} &= 150 \frac{(1-\delta_g)^2 \mu_g}{\delta_g d_p^2} + 1.75 \frac{(1-\delta_g) \rho_g |u_g - u_s|}{d_p} && \text{for } \delta_s > 0.74
 \end{aligned} \tag{7}$$

Coefficient ϖ depends on several flow and topological characteristics like the solid volume fraction, the particle diameter, the minimum fluidization velocity and the solid mass flow rate amount others. The last parameter indicates that this model was specifically formulated for circulating fluidized beds. So, the application of this model to confined fluidized beds is not possible with the present formulation. This model restriction must be overtaken, allowing the application of this model to fluidized bed systems (Wang et al., 2007). The coefficient ϖ is obtained by solving a energy minimization problem from a set of ten equations. The objective is to consider the drastic drag coefficient reduction originated during clustering. Detailed information about the EMMS model can be found in Yang et al. (2003, 2010). ϖ is a function of the local flow conditions, so the minimization problem must be solved for each computational cell of the domain. For industrial problems and also for laboratory ones, it has a high computational cost. So, ϖ can be assumed as constant by taking averaged values for the flow variables. Following, the functions of correction factor vs. voidage are described for this gas-solid system:

$$\begin{aligned}
 \varpi &= -0.576 + \frac{0.0214}{4(\delta_g - 0.7463)^2 + 0.0044} && \text{for } 0.74 \leq \delta_g \leq 0.82 \\
 \varpi &= -0.011 + \frac{0.0038}{4(\delta_g - 0.7789)^2 + 0.0040} && \text{for } 0.82 \leq \delta_g \leq 0.97 \\
 \varpi &= -31.8295 + 32.8295\delta_g && \text{for } 0.97 < \delta_g
 \end{aligned} \tag{8}$$

Figure 2 helps to magnify the difference between the three drag models considered in this work. As noted, the Wen and Yu and Gidaspow models have the same behavior for dilute systems, while for dense systems Gidaspow become greater. In contrast to the others two, for the EMMS model the coefficient K_{sg} is substantially reduced for dilute systems, thus representing the strong drag force reduction that take place under particle agglomeration or cluster formation.

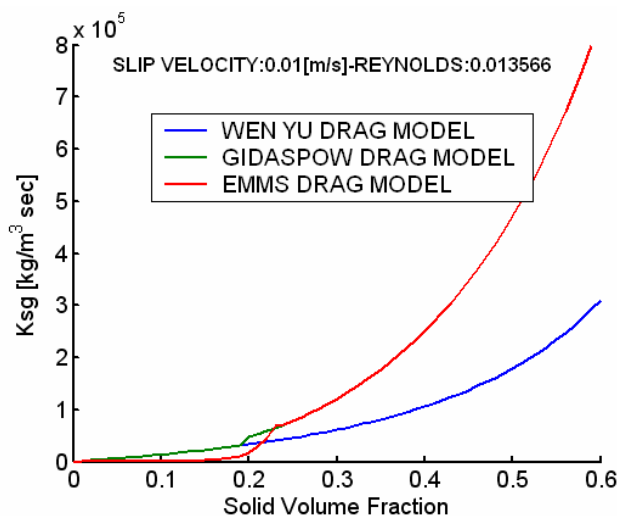


Figure 2: Interface momentum exchange coefficient K_{sg} for Wen and Yu, Gidaspow and EMMS models. Comparison for a slip velocity of 0.01 m/s

3 RESULTS AND DISCUSSION

3.1 Mesh convergence study

Figure 3 at the left shows results obtained by using three mesh grid sizes. Note that the mean and fine grids lead to similar results while the coarse one is far from the others two. That allows to conclude that the mean grid is suitable to perform simulations. As for the maximum time step it was set to 5×10^{-3} s. based on Gidaspow drag model results but it have to be reduced to 5×10^{-4} s. for the EMMS model drag simulations.

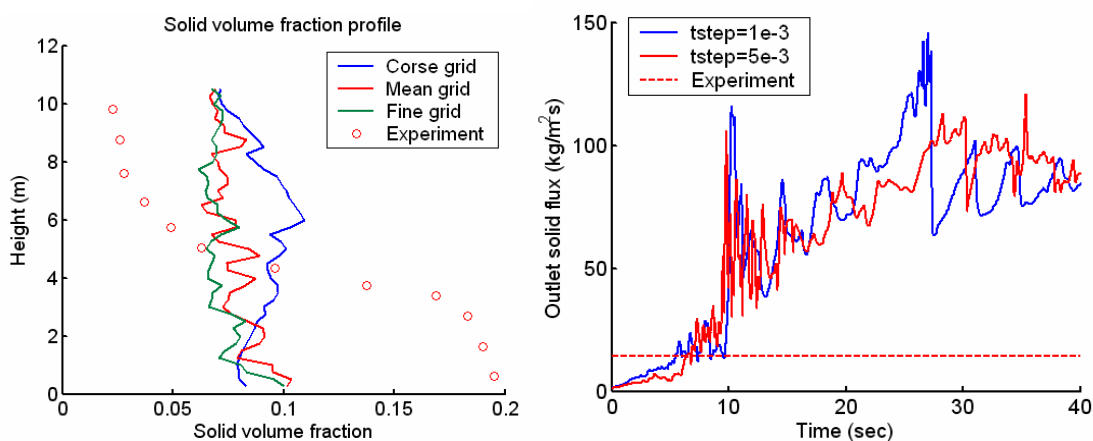


Figure 3: Mesh convergence study for Gidaspow drag model. Left: solid volume fraction profile for three grids (average from $t=70$ to $t=90$ s.). Right: mass flux rate at outlet for two time steps

Figure 4 shows pictures corresponding to Gidaspow results at two times for the three grids analyzed. Note that differences between the first and the others two grids are evident. On the other hand, results corresponding to the second and third grids seem to be similar, confirming that the use of the second grid is a suitable option to guaranty mesh independent results.

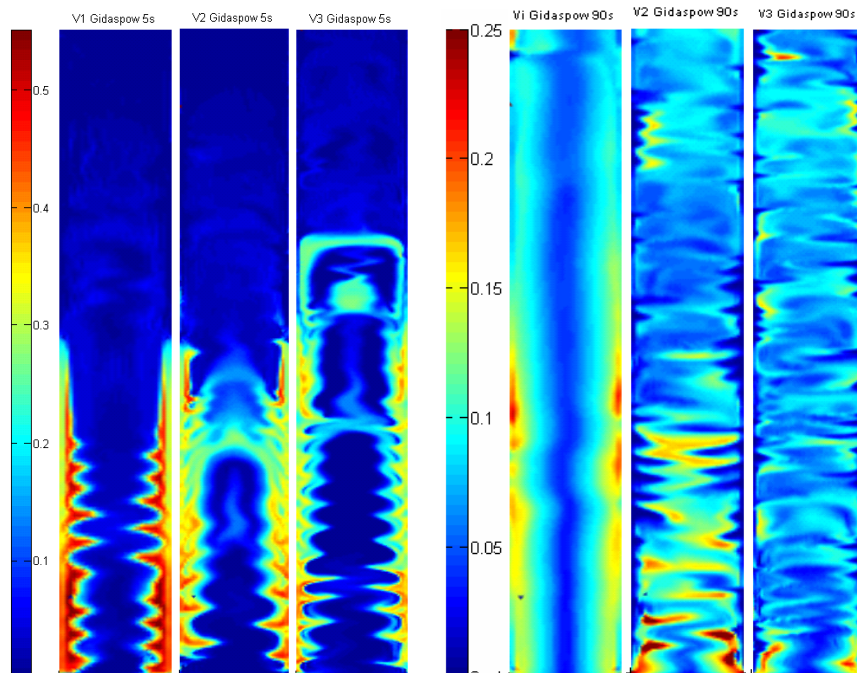


Figure 4: Mesh convergence study for Gidaspow drag model (time step= 5×10^{-3} sec) with three grids. Solid volume fraction at $t = 5$ sec and $t = 90$ sec

3.2 Drag model comparison

Figure 5 shows results obtained after 90 s. Comparing the results obtained with the three drag models, it is clear that the Wen and Yu and Gidaspow models are in close agreement. That can be explained by the fact that the solid volume fraction is mainly less than 0.2 as showed in Figure 4. As previously mentioned, for these solid concentrations both drag models are the same. Note that the solid concentration close the walls is almost zero along the riser. That behavior is contrary to the expected based on experimental observation and measurements. On the contrary, the EMMS model concentrates the solid phase at walls releasing the central channel for gas flowing. The other notorious difference is that for the EMMS model the most amount of solid is located at the bottom half of the riser.

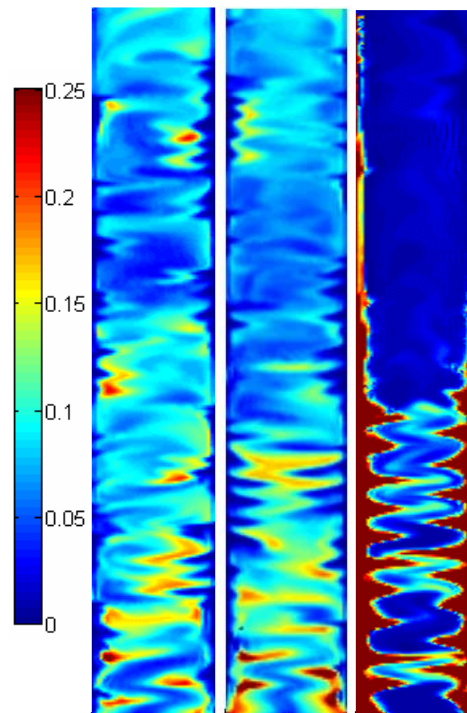


Figure 5: Solid volume fraction at $t = 90$ s. for Wen and Yu (left), Gidaspow (center) and EMMS (right) models

Figure 6 shows the comparison between the numerical and experimental data. On the left is drawn the solid mass flux rate of solid at the top outlet for the three drag models along with the experimental results. It is clearly noted that both Wen and Yu and Gidaspow models fairly overestimates the solid flux (around 6 times more), while the EMMS model is in good agreement with experimental data. The picture on the right shows the cross transversal average of the solid volume fraction profile along the longitudinal axis of the riser. Results were time averaged from eight instants between 70 s. and 90 s. The Wen and Wu and Gidaspow models estimated a solid concentration almost constant around 0.08 along the riser while the EMMS predict a significant concentration at the bottom side, fairly in agreement with the experimental data. Similar conclusions were found by Hartge et al. (2009) for a different gas-solid system and experimental layout.

In a more recent work, Yang et al. assessed the EMMS model with the same riser but for a solid mass flow rate of $165 \text{ kg/m}^2\text{s}$ (around ten times more) and inlet gas velocity of 15.5 m/s (around three times more), obtaining good agreement between numerical and experimental results (Yang et al., 2010). They also compared the pressure drop along the riser height finding that the EMMS estimation is fairly more in agreement with experimental data that the Gidaspow model one.

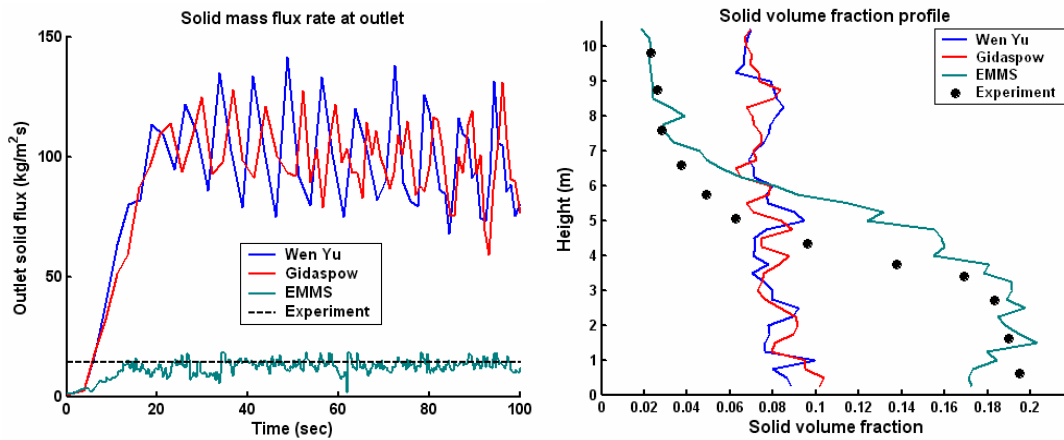


Figure 6: Left: solid mass flux rate at the outlet. Right: solid volume fraction profile along the y coordinate (average from $t=70$ to $t=90$ s.)

Figure 7 on the left shows the pressure drop along the riser for the three drag models. While the pressure drop profile is almost linear along the whole riser for the Wen and Yu and Gidaspow models. On the other hand, the EMMS model predict a quasi-linear pressure drop behavior until around the half of riser (6 m.), strongly reducing the pressure drop gradient after this height. Although there are not measurements for this particular system in literature, the current pressure profile is quite similar to those experimentally obtained for similar systems (Yang et al., 2010).

Figure 7 on the right shows the time evolution of the solid volume fraction profile. It is interesting to note that the required simulation time to reach the outlet solid flux steady state is quite shorter (see Figure 6 on the left) than the required to obtain a good agreement on the vertical solid distribution.

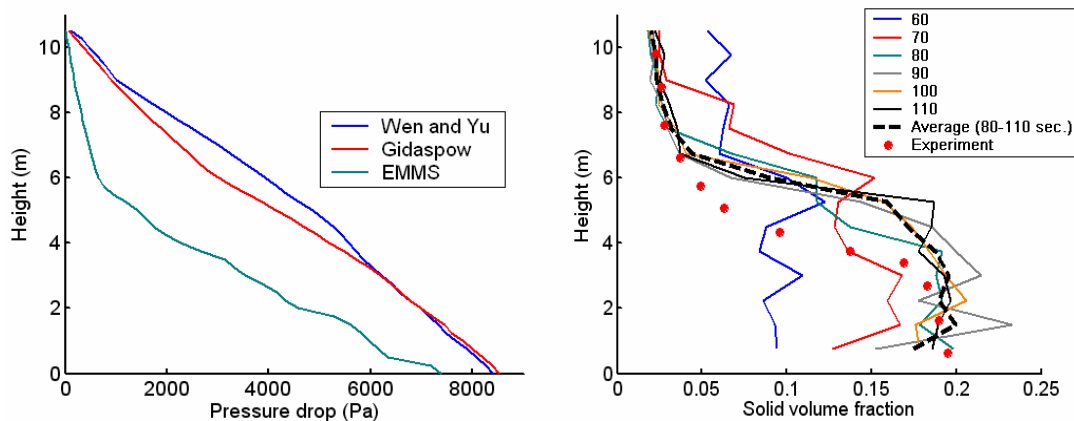


Figure 7: Left: Pressure drop after 100 s. for the three drag models. Right: Results from EMMS model with KTGF. Solid volume fraction profile along coordinate y for several times and the average

Unfortunately there is not experimental data about the solid distribution along the cross transversal axis of the riser. However, literature works report that solid concentrates at walls with scarce amount of solid at the central channel (Cruz et al., 2006; Almuttahir and Taghipour, 2008; Zhang et al., 2008; Hartge et al., 2009). This typical solid pattern was only obtained with the EMMS model as can be observed at Figure 8 on the left. Another expected solid behavior is the solid reversal flow that takes place close walls, causing negative vertical

velocities. Note from Figure 7 on the right that only the EMMS model reports significant reversal solid flow, also verifying the imposed no-slip wall boundary condition. Experimental data observing similar flow patterns were reported by Zhang et al. (2008). That allow to conclude that the EMMS estimations are more realistic that the corresponding to the other two models.

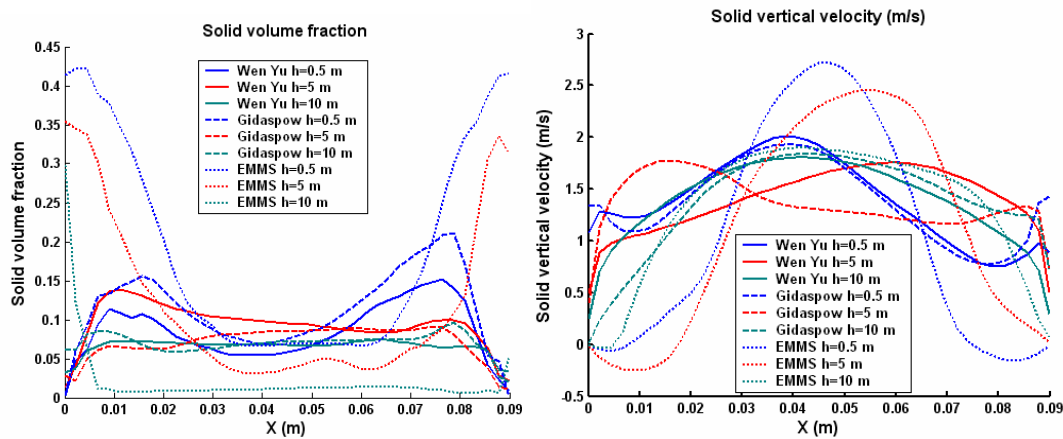


Figure 8: Average results from $t=70$ to $t=90$ s. Left: solid volume fraction profile along the x coordinate. Right: Solid vertical velocity along the x coordinate

3.3 Kinetic theory of granular flow

Figure 9 shows the results obtained with and without the KTGF for the Gidaspow drag model for the coarse grid (G_1). On the left picture are drawn the outlet flux curves for both cases. Results were time averaged, obtaining very much more smoothed curves. However, a significant reduction on oscillation can be observed for the model without KTGF. Besides, the overestimation is also reduced.

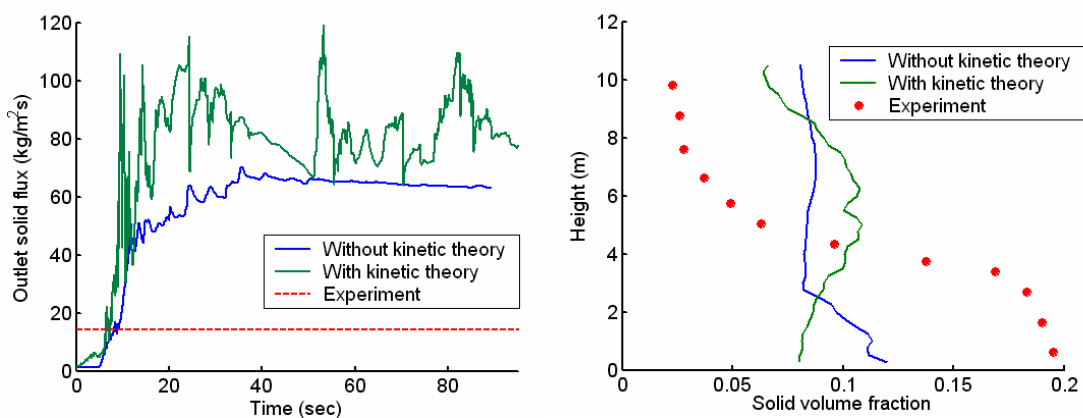


Figure 9: Results for Gidaspow model with and without kinetic theory of solid shear viscosity. Left: solid mass flux rate at the outlet. Right: solid volume fraction profile along the y coordinate (average from $t=60$ to $t=90$ s.)

Figure 10 compares results obtained with and without the KTGF for two times; 10 s. and 75 s. shows the results obtained with and without the KTGF for the EMMS drag model.

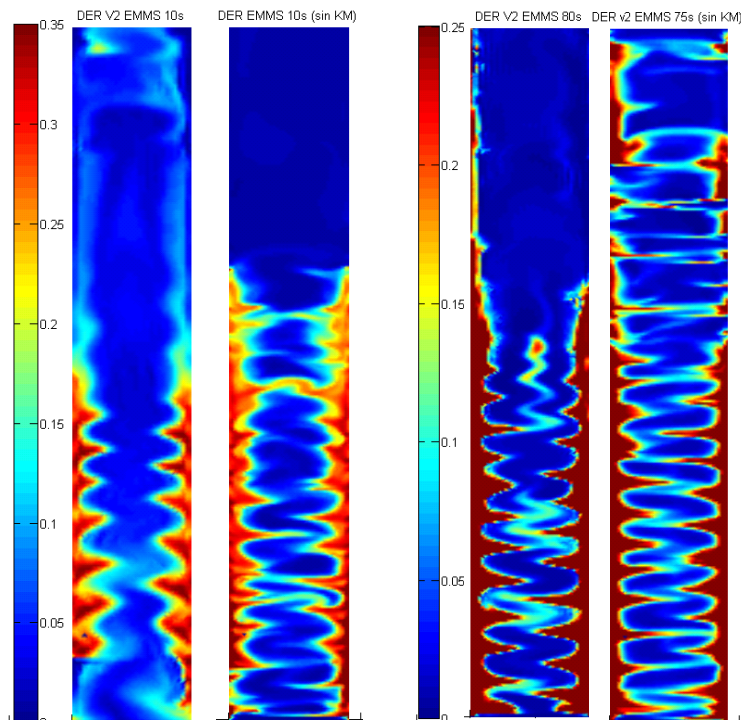


Figure 10: Solid volume fraction results from EMMS model with and without KTGF. Left: 10 s. Right: 75 sec

Figure 11 shows the influence of the KTGF on the outlet solid flux and the vertical distribution of solid. Note from the left picture that the outlet solid flux is almost the same for both simulations but significant instabilities arisen after 35 s. On the other hand, the vertical solid distribution is more drastically modified.

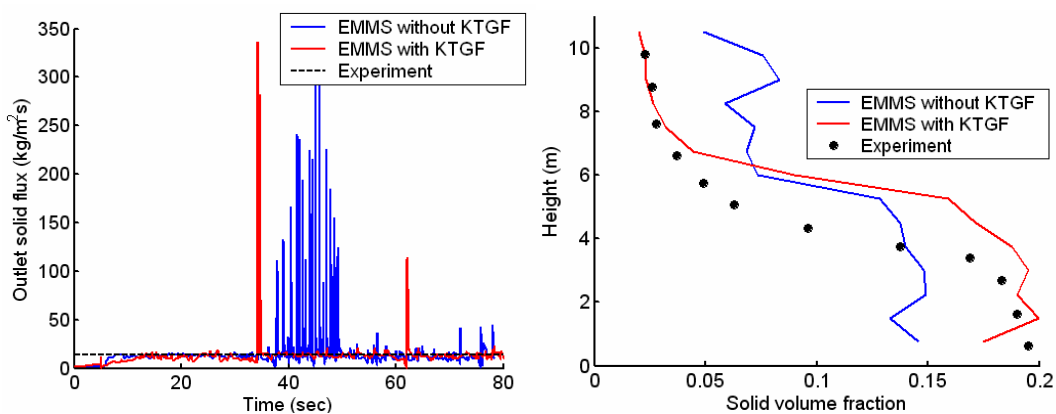


Figure 11: Results from EMMS model with and without KTGF (G_2 grid). Left: solid mass flux rate at the outlet. Right: solid volume fraction profile along the y coordinate (average from $t=60$ to $t=90$ s.)

It is quite difficult to conclude about the effect of the KTGF on result due to for the Gidaspow model it has adverse effects while for the EMMS model results are considerably improved.

3.4 Wall boundary condition

Three wall boundary conditions (WBC) were studied in this work, no-slip, free-slip and partial free-slip (free slip for particles and no-slip for gas phase). Results corresponding to the first WBC, that is no-slip, were presented in the previous sections.

As regards the free-slip and partial free-slip WBC, they were not suitable for simulations. The stability and convergence of simulations was drastically reduced by using either the free-slip and the partially free-slip wall conditions. Simulations could not be performed beyond 15 s. In order to improve the stability, the time step was modified without successful. Figure 12 shows the results after 10 s. for the three WBC. As previously noted for the no-slip WBC, particles locate close to the walls at the bottom half side of the riser, leaving a free central channel for gas upping (as an annular flow). As for the others two WBC, flow seems to follow a slug pattern with large gas and solid regions.

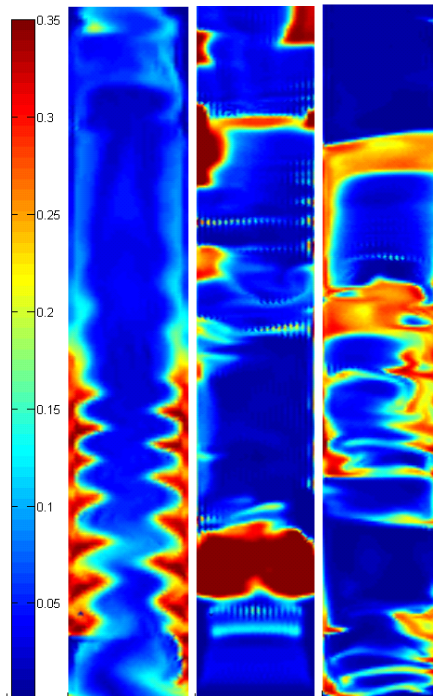


Figure 12: Solid volume fraction from EMMS model for the three WBC.
Left: no-slip. Center: free-slip. Right: partial free-slip

4 CONCLUSIONS

A two-phase turbulent flow in an experimental vertical riser was simulated by CFD. The most influencing simulation parameters were studied in deep, which lead to the following conclusions:

1- The currently most massively employed particle-gas drag models (Wen and Yu and Gidaspow) show to be inadequate for vertical riser applications where gas velocity is far from the minimum fluidization velocity and particle-cluster formation take place. Models overestimate the drag momentum exchange causing an overestimation of the solid mass flow rate. They also predict an almost constant solid profile along the riser axis. On the other hand, the EMMS model implemented shows good agreement with experimental data and more expected solid velocity and concentration profiles near walls.

- 2- Uses of the KTGF to quantify the particle-particle interaction along with the EMMS drag model had two effects; firstly improving the stability and convergence of simulations and secondly reaching to a better agreement between numerical and experimental results
- 3- The WBC election is crucial to successfully carry out simulations. In this sense, only the no-slip boundary condition for both phases allows to reach steady state results
- 4- The EMMS model shows to be a more suitable option to modeling CFB systems. Then, the present formulation could be modified and assessed to confined fluidized bed system applications.

Acknowledgement

Authors want to thanks to CONICET and ANPCyT (grant PICT 1645/2008) and UNL (grant CAI+D PI 65-333/2009).

REFERENCES

- Almutter A. and Taghipour F., Computational fluid dynamics of high density circulating fluidized bed riser: Study of modeling parameters. *Powder Technology*, 185:11-23, 2008.
- ANSYS-CFX 12 User Manual, 2008.
- Bahramian A., Kalbasi M. and Olazar M., Influence of Boundary Conditions on CFD Simulation of Gas-particle Hydrodynamics in a Conical Fluidized Bed Unit. *Int. J. of Chem. Reactor Eng.*, 7, A60, 2009.
- Cruz E., Steward F.R. and Pugsley T., New closure models for CFD modeling of high-density circulating fluidized beds. *Powder Technology*, 169:115-122, 2006.
- Drew D., and Passman S., Theory of Multicomponent Flow. Springer, New-York, 1998.
- Gauthier T., Current R&D Challenges for Fluidized Bed Processes in the Refining Industry. *Int. J. of Chem. Reactor Eng.*, 7, A22, 2009.
- Gidaspow D., *Multiphase flow and fluidization: continuous and kinetic theory descriptions*. Academic Press, 1994.
- Grace J.R., Bi H.T., Golriz M., Circulating fluidized beds, Handbook of fluidization and fluid-particle systems. Chap. 19, New York, 485-531, 2003.
- Hartge E., Ratschow L., Wischniewski R. and Werther J., CFD-simulation of a circulating fluidized bed riser. *Particuology*, 7:283-296, 2009.
- Huilin L., Gidaspow D., Bouillard J., and Wentie L., Hydrodynamic simulation of gas-solid flow in a riser using kinetic theory of granular flow., *Chem. Eng. J.*, 95:1-13, 2003.
- Mendez C., Nigro N., and Cardona A., Non-drag forces influence in numerical simulations of metallurgical ladles. *J. of Materials Processing Technology*, 160:296-305, 2005.
- Yang N., Wang W., Ge W. and Li J., CFD simulation of concurrent-up gas-solid flow in circulation fluidized beds with structure-dependent drag coefficient. *Chem. Eng. Journal*, 96:71-80, 2003.
- Wang Q., Zhang K., Sun G., Brandani S., Gao J. and Jiang J., CFD Simulation of Fluid Dynamics in a Gas-Solid Jetting Fluidized Bed. *Int. J. of Chem. Reactor Eng.*, 5, A112, 2007.
- Wang X.Y., Jiang F., Xu X., Fan B.G., Lei J. and Xiao Y.H., Experimental and CFD Simulation of Gas-Solid Flow in the Riser of Dense Fluidized Bed at High Gas Velocity. *Powder Technology*, In press, 2010.
- Zhang N., Lu B., Wang W. and Li J., Virtual experimentation through 3D full-loop simulation of a circulating fluidized bed. *Particuology*, 6:529-539, 2008.